Structural analysis of magnetic lineaments in Central-West Paraná Basin (RS, SC, PR)

Adelir José Strieder (Engenharia Geológica, CEng – UFPel, Pelotas – RS)
Sérgio Alfredo Buffon (GAT/UAA – Ministério Público do RS, Porto Alegre – RS)
Tomás Dalpiaz Strieder (Engenharia Geológica, CEng – UFPel, Pelotas – RS)

Abstract

This paper presents the magnetic lineaments analysis from the structural point of view. Projects 4023 and 4053 (ANP) from Central-west segment of Paraná Basin were under analysis. The low depth magnetic lineaments display two main orientations: EW and NW-NE. The NW-NE magnetic lineaments truncate the EW ones. Horizontal derivatives and directional filtering discriminate an orthogonal structural pattern for NW-NE lineaments. The analysis of field structural data makes possible to correlate these magnetic lineaments to 2 deformational episodes that took place in the Jurassic to Cretaceous period of the Paraná Basin. The magnetic sources were emplaced in the outer rim of domes and basins structures due to bi-directional constrictional stress regimes for both deformational phases.

Introduction

The Paraná Basin is a Phanerozoic intracratonic depression filled by sedimentary and volcanic rocks. Its main structural features include regional lineaments, arcs, and flexures (Fig. 1) that have been summarized by Almeida (1981), Zalán *et al*. (1991), and Zalán (2004). Details of such features were investigated using satellite imagery lineaments and fault plane trends (e.g., Soares *et al*., 1982; Zerfass *et al*., 2005; Reginato & Strieder, 2006; Strugale *et al*., 2007; Machado *et al*., 2012; Nummer *et al*., 2014; Jacques *et al*., 2014), geophysical lineaments (e.g., Ferreira, 1982; Ferreira *et al*., 1989; Quintas, 1995).

Paleostress analysis were conducted by Riccomini (1995) and Strugale *et al*. (2007), who proposed a strike-slip stress regime to and distinguished the deformational phases from the Permian to Holocene units of the Paraná Basin.

Continuing fieldwork activities have been conducted in the Serra Geral Fm. (from 1995 on), describing and analyzing volcanic and deformational structures. The structural investigations lead Strieder *et al*. (2015) to propose that both deformational phases (NS-EW, and NE_NW) were developed under regional bi-directional constrictional ($\sigma_1 \geq \sigma_2 >> \sigma_3$) stress regimes Jurassic to Cretaceous periods in the Paraná Basin.

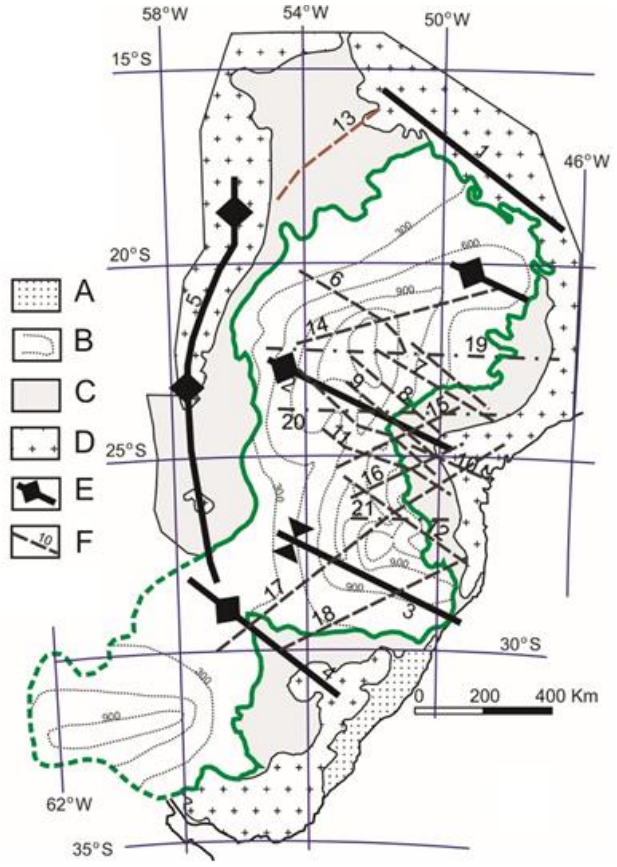

Figure 1 – Geological sketch of the Paraná Basin and its main structural features (modified from Leinz et al. 1968; Zalán et al. 1991). Legend: A) Quaternary sediments. B) Serra Geral Fm.; dotted lines show the actual thicknesses of the volcanic rock piles. C) Paleozoic to Mesozoic sedimentary rocks. D) Basement rocks. E) Structural highs, arches, and synclines. F) Main fault zones (numbered): 1) Alto Parnaíba high; 2) Ponta Grossa Arc; 3) Torres Syncline; 4) Rio Grande Arc; 5) Asunción Arc; 6) Guapiara; 7) Santo Anastácio; 8) São Jerônimo–Criúva; 9) Rio Alonso; 10) Cândido de Abreu–Campo Mourão; 11) Rio Piquiri; 12) Caçador; 13) Transbrasiliano; 14) Araçatuba; 15) Guaxupé; 16) Jacutinga; 17) Lancinha–Cubatão; 18) Blumenau–Soledade; 19) Mogiguaçu–Dourados; 20) São Sebastião; 21) Taquara Verde.

Both deformational phases characterized by Strieder *et al*. (2015) produced orthogonal non-cylindrical folds (elliptical domes and basins). The second deformational phase produced the prominent NE arc-synclines

sequence (Ponta Grossa Arc, Torres Syncline, and Rio Grande Arc) close to eastern continental border.

The bi-directional constrictional stress regimes for both deformational phases reconcile fault-slip data and the orthogonal veins and dykes' patterns as recoded in fieldworks. Strieder *et al*. (2015) showed that these structural features are due to second order (local) stress field resulting from stress drop in the hinge zone of the regional elliptical dome-basin structures.

The aim of this paper is to present the results of a structural analysis on geophysical maps considering the results presented by Strieder *et al*. (2015), and continuing fieldworks in the Paraná Basin.

The geophysical maps were developed from aeromagnetometric surveys (4023 and 4053) contracted by PETROBRAS (1980 and 1989, respectively).

Methods of data processing and fieldwork records

The processing and analysis of the aeromagnetometric databases (4023 and 4053) were mainly performed in OASIS-MONTAJ environment (GEOSFT®).

The processing flow of the geophysical data is summarized in figure 2. Since Rio Iguaçu Project (4023) flight lines were surveyed at 500 m high, while West Paraná Basin Project (4053) were flown at 1000 m high, is was necessary to perform Upward Continuation of 4023 Project data to make them compatible with 4053 Project data. After that, both databases were integrated and Microlevelling and Directional Cosine Filter could produce the integrated magnetometric map for the Central-western border of the Paraná Basin in Brazil (Figure 3).

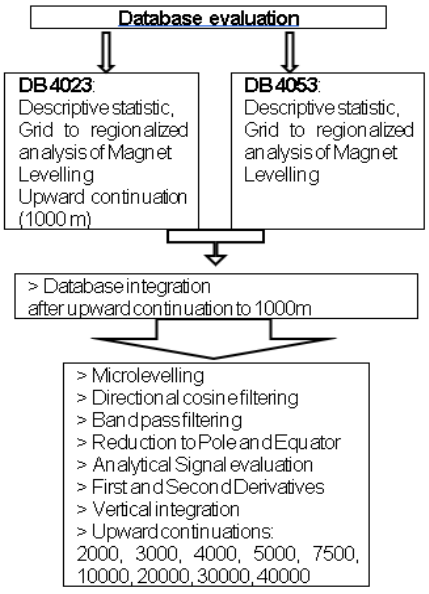

Figure 2 – Flowchart for central-west Paraná Basin magnetometric databases (4023 and 4053) processing.

The following magnetometric data processing steps (Fig. 2) were, then, applied to depict structural features of the Paraná Basin at different depths.

The fieldworks have been carried on continuously in different areas of the Paraná Basin, and are designed to accomplish specific purposes in each one. The recorded data includes description and orientation of: lithology, primary volcanic / sedimentary structures, dykes, veins, fractures, fault slip data, and any other geological feature observed in outcrops.

Magnetic structures characterization

Some of the magnetometric maps resulting from processing workflow are presented to enable the characterization of low depth magnetic lineaments. These magnetic lineaments may show greater structural significance for uppermost stratigraphic units of the Paraná Basin and to Mesozoic deformation than do the deeper ones.

Figure 3 shows the remanescent magnetic field (A), its first vertical derivative (B) and its regional component after Gauss filtering (C). Figures 3A and 3B clearly show a series of EW and NW-NE trending magnetic lineaments. The low depth magnetic source lineaments (Figure 3B) does show intersecting relationships: the higher amplitude NW and NE ones truncate the EW ones.

Figure 3C shows a deeper magnetic structure than figure 3B, and also shows that lineaments. However, it shows NW trending lineaments that seems to be related to block tilting and vertical movements rather than strike slip displacement.

Figure 4 shows the Tilt Angle Derivative map for Remanescent Magnetization, to investigate the magnetic sources at low depth. This figure emphasized the EW, NW and NE lineaments, but do not enable an adequate analysis since lineaments directions are superposed.

The filtering procedures, then, were performed to discriminate and emphasize between lineaments, in order to better understand their structural control.

Figure 5 shows horizontal derivates applied onto Remanescent Magnetization map. Figure 5A show horizontal derivative in Y direction; it emphasized the EW magnetic lineaments, some of them displaying high amplitude. Figure 5B shows the X horizontal derivative for Remanescent Magnetization and, on the other hand, displays an orthogonal lineament pattern (NW and NE lineaments). Figure 5A also shows that high amplitude NW magnetic lineaments truncate the EW low amplitude ones.

A FFT filtering procedure was also applied in each individual flight line to overcome levelling problems. The high-pass (< ~1000 m) results were then interpolated to give rise a levelled high-pass remanescent magnetization map (Figure 6A). This high-pass filtered magnetic map displays, more effectively, the EW trending magnetic lineaments.

Directional cosine filtering was applied onto FFT filtered map (Figure 6A). The filtering directions were selected along and across flight lines to prevent artifacts.

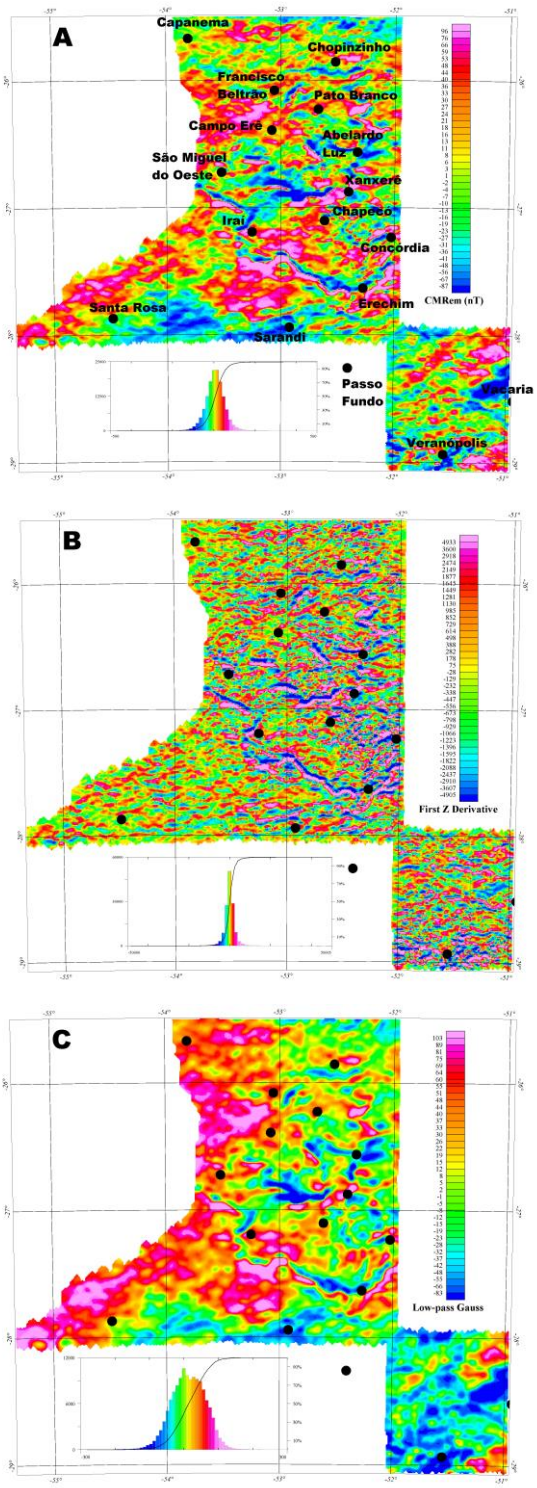

Figure 3 – Magnetometric maps of the West-central Paraná Basin. A) Remanescent Magnetization (DGRF_1990); B) First vertical derivative of the previous map; C) Low-pass (Regional) gaussian filtered Remanescent Magnetization map.

The across flight line directional cosine filtering (Figure 6B), as expected, clearly showed the EW magnetic lineaments. It can be compared to results of Y-direction horizontal derivative (Figure 5A), but do not present the NW and NE magnetic lineaments.

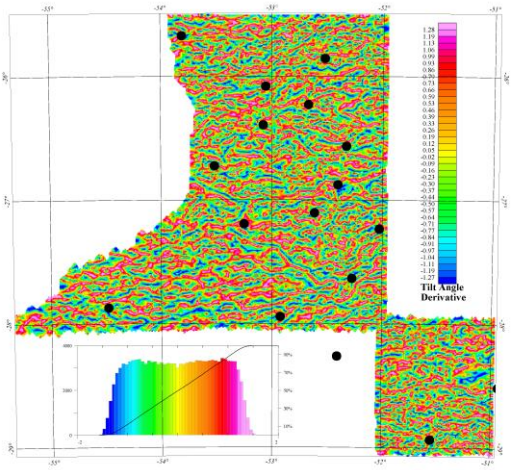

Figure 4 – Tilt Angle Derivative map for Remanescent Magnetization in the W Paraná Basin.

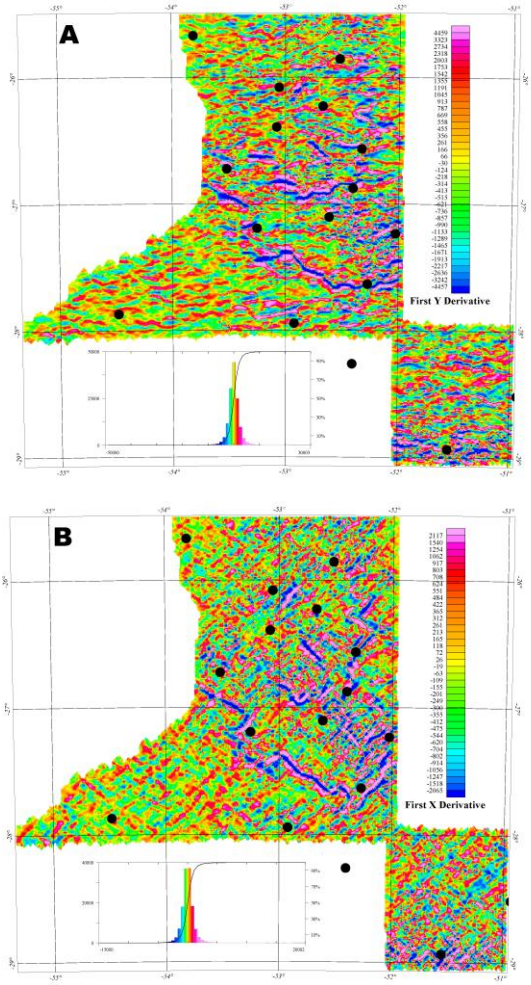

Figure 5 – Horizontal derivative maps for Remanescent magnetization. A) Y-direction derivative; B) X-direction derivative.

The along flight line directional cosine filtering (Figure 6C), on the other hand, does reinforce the NW and NE orthogonal magnetic lineament pattern. The structural pattern depicted in figure 6C is similar to, but better characterized than that emerging from horizontal X derivative (Figure 5B).

Figure 6A presents some dipolar circular magnetic features; the most evident is located few kilometers NE from Sarandi City. After directional filtering (Figures 6B and 6C), such features collapse to an orthogonal pair of dipolar ones. The dipolar feature NE of Sarandi City corresponds to an intrusive magmatic body on Serra Geral basalts, as can be seen in a crushed stone quarry located in that area.

Field investigations and discussions

The EW, NE and NW magnetic lineaments distinguished in figures 3, 5 and 6 are all compatible to structures described and analyzed by Strieder *et al*. (2015). The NW and NE magnetic lineaments truncating the EW ones also corroborates field observations as characterized by Strieder *et al*. (2015).

The first deformational phase distinguished by Strieder *et al*. (2015) developed an orthogonal dike pattern in the outer rim of large scale non-cylindrical buckled folds. However, local scale buckling folds of this deformational phase should develop the same orthogonal pattern, as had been recorded by fieldwork (Figure 7). The EW-NS orthogonal dike pattern was recorded in Serra Geral volcanics of Salto do Jacuí region (Heemann, 2005), but it is also recorded in lower Rio do Rasto (Figure 7A). This orthogonal dike pattern in sedimentary units is closely related to oblate boudins of thin sandstones packed between shale layers (Figure 7B).

The second deformational phase characterized by Strieder *et al*. (2015) also developed an orthogonal fracture pattern filled by veins and dikes, which was better recorded in the Caxias do Sul - Veranópolis region (Reginato & Strieder, 2006). However, this orthogonal fracture pattern is oriented NW-NE, and records a clockwise rotation of the stress field. In Cascavel (PR) region, north of this surveyed area, the NW-NE orthogonal vein pattern is also observed (Figure 8).

The orthogonal fracture pattern is developed in the outer rim of folds produced by bi-directional constrictional stress regime (Strieder *et al*., 2015). These fracture patterns, then, represent local (second order) stress field due to buckling mechanism.

The inner rim of these regional buckles, on the other hand, encompasses additional constrictional deformation. The local scale deformational features in the inner rim of such buckles should be represented by folds, thrust and/or reverse faults.

Figure 9 presents some of the local scale deformational features developed in the inner rim of regional buckles, arcs and synclines in the Paraná Basin.

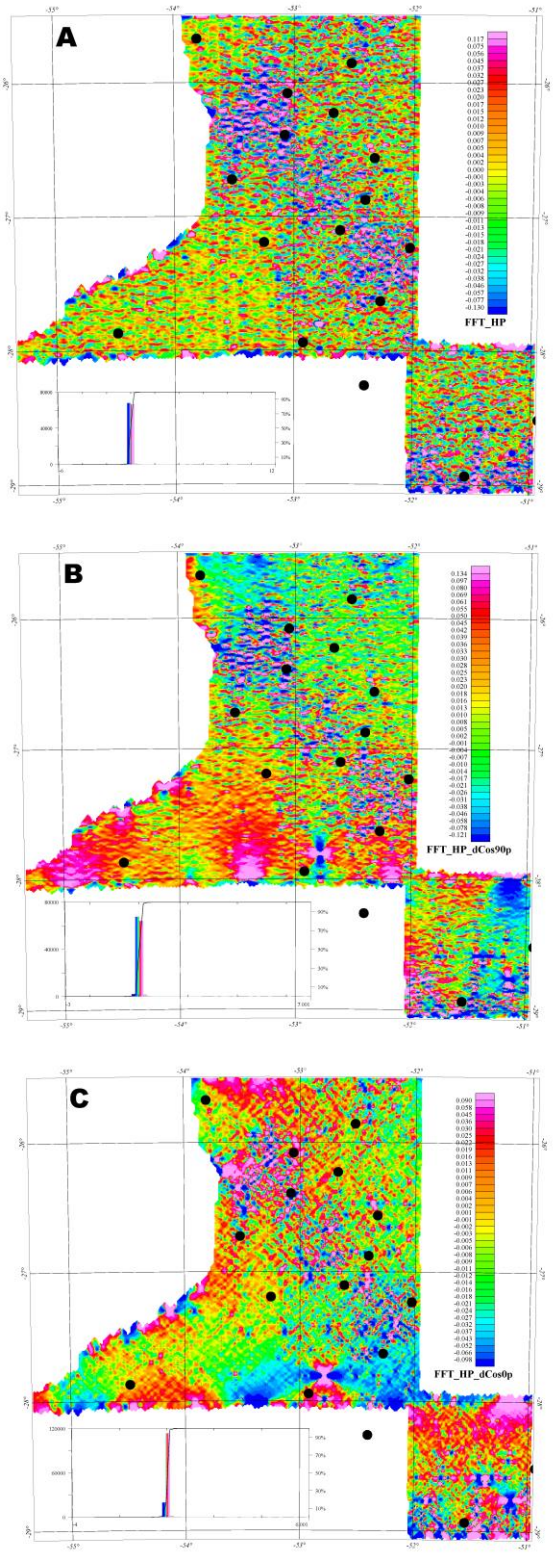

Figure 6 – FFT high-pass magnetometric maps (A), across flight line directional cosine filtered (B), and along flight line directional cosine filtered (C).

Figure 7 – (A) EW-NS orthogonal sandstone dike pattern, and (B) Boudins on sandstone packed between thicker shale layers developed upon Rio do Rasto Fm. in Rio Grande do Sul.

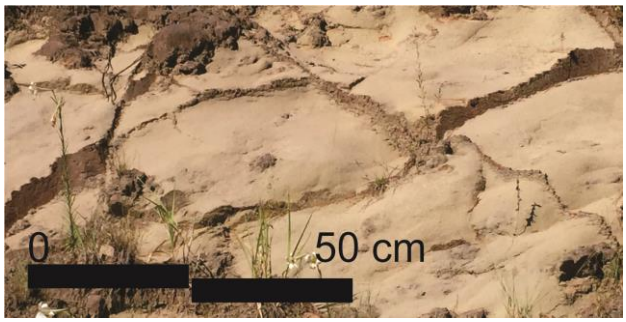

Figure 8 – Orthogonal vein pattern in the Cascavel region (PR), developed in the second deformational phase.

Figure 9A shows chevron style folds recorded in the lower bituminous shale, Irati Fm., of the PETROSIX mine (São Mateus do Sul, PR). Some of these chevron folds are closely related to reverse faults. It is noteworthy, however, that upper bituminous shale unit do have boudins developed upon calcareous layers. It can be proposed, then, that the neutral surface of the regional buckle is in the sedimentary rocks midway between the upper and the lower bituminous shale units.

Boudins are also recorded in thin mechanical competent layers between lower and upper coal units of the Rio Bonito Fm. This local scale structural feature is observed in the outer rim of the Torres Synclinal, Carbonífera Catarinense Mine, Lauro Müller region (SC).

Figure 9B shows conjugated thrust faults, opposite dip, duplicating layering of the Palermo Fm. Both thrust faults show front head folds developed in its hanging-wall. The main fault, dipping northeast, has >20 m of displacement, measured from footwall cut to the front head fold.

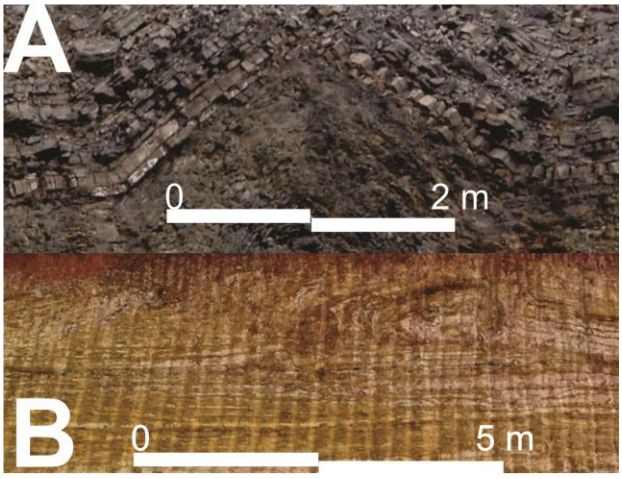

Figure 9 – Local scale (second order) structural features in Paraná Basin. A) Chevron style folds in the lower bituminous shale, Irati Fm. (PETROSIX mine, São Mateus do Sul, PR); B) Conjugated thrust faults in the rhythmic layering of Palermo Fm. (Pantano Grande, BR-290, RS)

Final discussion and conclusions

Low depth magnetic lineaments show strong structural control in West-central Paraná Basin. They represent magnetic sources emplaced in the Serra Geral Fm. The mechanical properties of the volcanic rocks favor fracture development during buckling processes, as pointed out by Strieder *et al*. (2015).

The NW-NE orthogonal pattern developed by low depth magnetic lineaments does correspond well to orthogonal T fractures described in the outer rim of domes and basins, and arcs and synclines of the D_2 deformational phase (Strieder *et al*., 2015).

The EW low depth magnetic lineaments represent incomplete pattern of orthogonal T fractures described in the outer rim of domes and basins of the D_1 deformational phase (Strieder *et al*., 2015).

The EW magnetic lineaments are not completed with NS ones since NS lineaments would lay along flight lines. This parallelism may be the source for microlevelling problems detected in processing BDs. And, levelling and

microlevelling procedures would rule out these NS lineaments.

The EW magnetic lineaments are truncated by NW-NE ones (Figures 3B and 5A). This record also corroborates the observations and structural characterization of deformational phases: D_1 (NS-EW orthogonal fracture pattern), and D_2 (NW-NE orthogonal fracture pattern).

The EW and NW-NE magnetic lineaments can be traced to deep source structures. But they are completely developed as low depth magnetic sources structurally controlled by orthogonal T joints patterns developed in the outer rim of folds related to D_1 and D_2 deformational episodes.

The structural analysis based on magnetometric maps and fieldwork data showed an interplay between second and first order deformational structures. In fact, second order structures depend on deformational mechanisms and on structural position of the first order ones.

In this way, the exposure of connected conjugate thrust faults (Figure 9C) is a rare example of local scale deformational feature that can be interpreted in conflicting ways if observed in separate, far apart outcrops. The interpretations of the structural features discussed above can pose tectonic problems if they are taken as first order instead of second order structures.

Acknowledgments

The authors wish to thank ANP (Agência Nacional do Petróleo), that kindly made available the aeromagnetometric databases for surveys 4023 and 4053 (PETROBRAS 1980 and 1989, respectively).

The authors also thanks Eng de Minas Gianfrancesco O. Cerutti (PETROSIX), Eng de Minas Carlos A. A. da Silveira and Eng de Minas Cristhian Paludo (Carbonífera Catarinense), and Eng de Minas Douglas R. Loureiro (Companhia Riograndense de Mineração, Candiota, RS), who made possible fieldwork in mine sites.

References

Almeida FFM. 1981. Síntese sobre a tectônica da Bacia do Paraná. IN: Simp Regional de Geologia, 3, v1, 1–20

Ferreira FJF. 1982. Integração de Dados Geofísicos e Geológicos: Configuração e Evolução Tectônica do Arco de Ponta Grossa. Dissertação de Mestrado, PPG em Geoquímica e Geotectônica, IG-USP, 273 pp.

Ferreira FJF; Monma R; Campanha GAC; Galli VL. 1989. An estimate of the degree of crustal extension and thinning associated with the Guapiara Lineament based on aeromagnetic modelling. Boletim IG-USP, 20, 69–70.

Heemann R. 2005. Modelagem exploratória estrutural e tridimensional para a prospecção dos depósitos de ágata do Distrito Mineiro de Salto do Jacuí (RS). PhD thesis, PrPG em Engenharia de Minas, Metalurgia e Materiais, UFRGS, 163 pp.

Jacques PD; Machado R; Oliveira RG; Ferreira FJF; Castro LG; Nummer AR. 2014. Correlation of lineaments (magnetic and topographic) and Phanerozoic brittle structures with Precambrian shear zones from the basement of the Paraná Basin, Santa Catarina State, Brazil. Bra J Geol, 44, 39–54.

Leinz V; Bartorelli A; Isotta CAL. 1968. Contribuição ao estudo do magmatismo basáltico Mesozóico da Bacia do Paraná. Academia Brasileira de Ciências, 40, 167–181.

Machado R; Roldan LF; Jacques PD; Fassbinder E; Nummer AR. 2012. Tectônica transcorrente Mesozoica-cenozóica no Domo de Lages – Santa Catarina. Revista Brasileira de Geociências, 42, 799–811.

Nummer AR; Machado R; Jacques PD. 2014. Tectônica transcorrente mesozoica/cenozoica na porção leste do Planalto do Rio Grande do Sul, Brasil. Pesquisas em Geociências, 41, 121–130.

Quintas, M. C. L.: O embasamento da Bacia do Paraná: reconstrução geofísica de seu arcabouço. Tese de Doutoramento, PPG em Geofísica (IAG-USP), São Paulo (SP), 213 pp., 1995.

Reginato PAR; Strieder AJ. 2006. Caracterização estrutural dos aquíferos fraturados da Formação Serra Geral na região nordeste do Estado do Rio Grande do Sul. Revista Brasileira de Geociências, 36, 13–22.

Riccomini, C. 1995. Tectonismo gerador e deformador dos depósitos sedimentares pós-gonduânicos da porção centro-oriental do Estado de São Paulo e áreas vizinhas. Tese de Livre Docência, IG-USP, 100 pp.

Soares AP; Barcellos PE; Csordas SM; Mattos JT; Balieiro MG; Meneses PR. 1982. Lineamentos em imagens de Landsat e Radar e suas implicações no conhecimento tectônico da Bacia do Paraná. IN: Simp. Bras. Sens. Remoto, 2, 143–168.

Strugale M; Rostirolla SP; Mancini F; Portela Filho CV; Ferreira FJF; Freitas RC. 2007. Structural framework and Mesozoic–Cenozoic evolution of Ponta Grossa Arch, Paraná Basin, southern Brazil. J S Am Earth Sci, 24, 203–227.

Strieder AJ; Heemann R; Reginato PAR; Acauan RB; Amorim VA; Remde MZ. 2015. Jurassic–cretaceous deformational phases in the Paraná intracratonic basin, southern Brazil, Solid Earth Discuss, 7, 1263-1314, doi:10.5194/sed-7-1263-2015.

Zalán PV. 2004. Evolução Fanerozóica das bacias sedimentares brasileiras. IN: Neto VM; Bartorelli A; Carneiro CR; Brito-Neves BB. 2004. A Geologia do Continente Sul-americano, Editora Beca, pp. 595–613.

Zalán PV; Wolff S; Astolfi MAM; Vieira IS; Conceição, JCJ; Appi VT; Neto EVS; Cerqueira JR; Marques A. 1991. The Paraná Basin, Brazil. AAPG Memoir., 51, 681–707.

Zerfass H; Chemale Jr F; Lavina ELC. 2005. Tectonic control of the Triassic Santa Maria Supersequence of the Paraná Basin, Southernmost Brazil, and its correlation to the Waterberg Basin, Namibia. Gondwana Res, 8, 163–176.